A numerical study of H_2-air rotating detonation combustor

Shashank Yellapantula,* Venkat Tangirala, Kapil Singh and Joel Haynes
General Electric (GE), Global Research Center (GRC)
Niskayuna, NY, USA

1 Introduction

Recent advances in pressure gain combustion have highlighted the performance potential of rotating detonation engine technology for propulsion and energy generation applications [1–3]. Specifically, the rotating detonation combustion (RDC) architecture overcomes some of the typical shortfalls of pulsed detonation type combustor systems. RDC systems do not require any moving parts and have significantly less unsteadiness in the combustor exhaust gases. Advances have been reported [1–3] in obtaining robust detonations, and using several fuels including hydrogen, ethylene and other hydrocarbons in oxygen-enriched environment and air.

One of the major technical challenges encountered while developing RDC for propulsion or energy generation applications can be relatively poor combustion efficiency (relative to deflagration based combustion) and resulting high levels of emissions especially in combustors with smaller residence times. In the present computational study, an attempt has been made to improve our understanding of mechanisms, such as fuel-air mixing responsible for pollutant emissions and poor combustion efficiency. The primary motivation for this computational research stems from the need to perform trade studies of RDC to understand the effect of operating and inlet parameters on the RDC performance metrics.

2 Configuration details

All the numerical studies shown in this study were performed on the 152.4 [mm] (6 [inch]) diameter AFRL atmospheric RDC configuration [4, 5]. Figure 1, shows a cross-section of this configuration. As shown in the Fig. 1, air is injected upstream in the plenum and enters the annulus channel through a bellmouth shaped air gap with a throat width of 1.78 [mm]. Fuel is injected into the fuel plenum and enters the annulus channel through 120 cylindrical fuel holes with a diameter of 0.89 [mm] each. The inner and the outer diameters of the channel annulus are 138.7 [mm] and 153.9 [mm]. An initiator tube with a diameter of 6.35 [mm] (0.25 [inch]) and $L/D = 8$ is attached the cylindrical annulus tangentially. Numerical simulations of this RDC configuration have been the subject of several recent research investigations [6, 7].

The domain shown in Fig. 1 is discretized using 24 million cells. Approximately 85% of the elements are hexahedral and the rest of the elements are comprised of triangles and prisms. The mesh elements are clustered in each of the 120 fuel holes, air gap and the channel annulus. The upstream and downstream plenums are progressively coarsened to optimize the total number of elements and thus the computational cost.

3 Numerical Simulation Setup

ANSYS FLUENT is used to perform all the simulations described in this study. A pressure based Navier-Stokes solver [8] is used to solve the compressible set of equations, to compute all the simulations described in this study.

*Currently working at National Renewable Energy Laboratory (NREL), Golden, Colorado, USA.

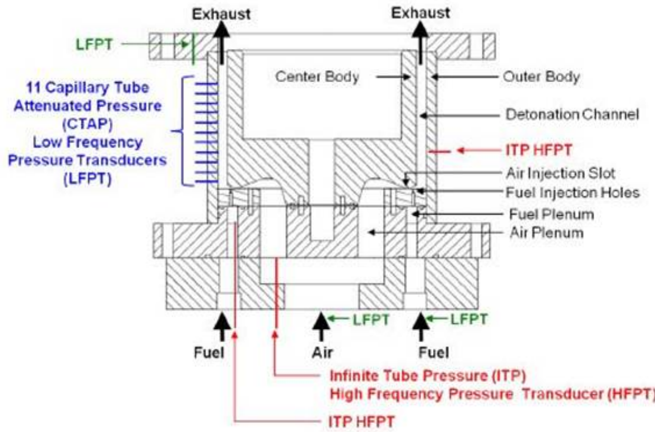

Figure 1: AFRL 152.4 [mm] (6 [inch]) RDC configuration [4]

An ideal gas equation of state is used as the constitutive relation. An Unsteady Reynolds Averaged Navier Stokes (URANS) model based on the $\kappa - \epsilon$ model is used to provide closure to the unsteady turbulent flow equations. Standard wall functions are used to resolve the near-wall turbulence. Momentum and energy equations are solved using the second order central difference and upwind formulations respectively. Bounded second order implicit formulation was used to discretize equations in time. A constant time-step of 5e-8 [s] is used to resolve the unsteady flow.

Finite rate chemistry with no turbulent closure assumption is employed to resolve the reacting flows in the combustor. With this assumption unsteady advection-diffusion-reaction equations are solved for the all species in the chemical mechanism. A 10 species, 21 reaction mechanism [9] is used to describe the chemical kinetics of the H2-Air system. Mass flow inlet boundary conditions are applied to both air and fuel inlets. In order to model the quiescent atmospheric conditions an outlet plenum is added to the geometry and constant pressure, P_{out} = 101325.0 [pa] is enforced as boundary condition. Adiabatic wall boundary condition are applied to all wall surfaces. The air and fuel flow rate along with the global equivalence ratio for the two cases described this study are listed in the following table, Table 1. These boundary conditions are chosen to match the boundary conditions prescribed in the experiments performed at AFRL [4].

Steady non-reacting RANS solution of mixing between fuel and air streams is used as the initial conditions for the unsteady URANS solution. In order to initiate a detonation in the channel, the initiator tube is filled with stoichiometric H2-O2 mixture and an ignition kernel is initiated at the end of the initiator. The details of ignition process and the setting up of detonation fronts in the annulus channel are discussed in more detail in Sec. 4.

Table 1: Simulation Boundary conditions

Case	Air flow rate [kg/s]	Fuel flow rate [kg/s]	Global Equivalence ratio
1	0.63	0.018	1.01
2	0.86	0.025	1.00

4 Results

Ignition

As mentioned in the Sec. 3, in order to initiate detonation in the annulus channel, the ignition procedure in the experiments in closely reproduced in the simulations. An initiator tube is tangentially inserted into the channel annulus. At the start of the unsteady simulation the initiator tube is filled with $H_2 - O_2$ mixture in stoichiometric proportions. An ignition kernel in form of post detonation Chapman-Jouguet (CJ) temperature, pressure and species is initialized in a 2.5 [mm] radius spherical pocket. Initially two high pressure waves traveling in opposite directions are generated. Eventually the leading detonation front reflects off the inner annulus channel wall, developing into two fronts traveling in opposite directions. Similar behavior of detonation front initiation in the annulus channel was observed in experiments at AFRL [11]. In all the simulations discussed in this study typically after 2-3 rotations one of the waves is observed to die out leaving a uni-directional traveling front in the annulus channel.

Fill height and multiple fronts

From the Table. 1, it can be observed that in Case-2, as compared to Case-1, higher amount of air flow and correspondingly fuel flow are flown through the annulus channel. As a consequence of the higher flow rate of fuel-air mixture the fill height in the annulus channel is higher, leading to the bifurcation of one detonation front into two detonation fronts. Existence of multiple detonation fronts in the annulus channel in turn results in shorter fill height due to reduced charge refresh time. A detailed study explaining the precise mechanism behind bifurcation and formation of two detonation waves will be presented in future.
Figure 2, shows the instantaneous pressure contours on a constant radius section (r = 73 [mm]) from simulations of Case-1 and Case-2. Across the detonation front a steep rise in pressure is observed. Additionally an oblique shock wave attached to the detonation front and a shock wave reflected off the annulus walls is observed downstream of the detonation front. Shock wave reflection off the annulus walls, as observed in Fig. 2, has been studied in great detail in [10].
Figure 3 compares the height of the detonation front obtained from numerical simulations of Case 1 & 2. Instantaneous contours of normalized reaction heat release in [J m^3/(kg s)] are plotted on a log scale on the constant radius (r = 72 [mm]) section of the channel annulus. As mentioned previously due to the existence of multiple fronts resulting in higher wave frequency and therefore a shorter refresh/fill time period. Qualitatively similar behavior is observed in OH^* chemiluminescence measurements conducted at AFRL. For the air flow rates corresponding to Case 2, refer table 1, two detonation fronts and a shorter detonation height were observed in the experiments [4]. In terms of wave frequency, simulation are observed to over-predict when compared against experiments, Table 2. Simulations in the current study were performed using adiabatic wall boundary conditions and therefore the impact of heat loss to walls is not captured. Other numerical studies have also noted the importance of heat loss in capturing the wave frequency [6]. The impact of heat loss on wave frequency will be studied in detail in the future studies.

Table 2: Wave frequency comparison between experiments and simulations

Case	Experiments [kHz]	Simulations [kHz]
1	3.78	4.16
2	7.37	8.02

Mixing and detonation stabilization

The RDC configuration as shown in Fig. 1 is an inherently non-premixed set up. Therefore detonation stabilization, combustion efficiency, and emissions production are strongly dependent on quality of fuel-air mixing. In order to study the fuel-air mixing in detail, a passive scalar based on conservation of element fractions commonly known as Bilger mixture fraction [12], Z, is generated. This passive scalar provides an excellent measure of local fuel-air equivalence ratio in a reacting simulation framework. Figure 5a shows the instantaneous contours of Bilger mixture fraction on a cross section of the annulus channel. The air flow from the plenum mixes with fuel flow in the throat section before entering the annulus channel. Due to the fuel injection at the point of highest air flow velocity (throat section), the fuel air mixture is concentrated towards the outer wall of the annulus channel. This preferential concentration of fuel-air mixture towards the outer wall also results in formation of a recirculation bubble towards the inner channel annulus wall. Additionally due to this bubble, fuel rich ligaments are observed to break off from

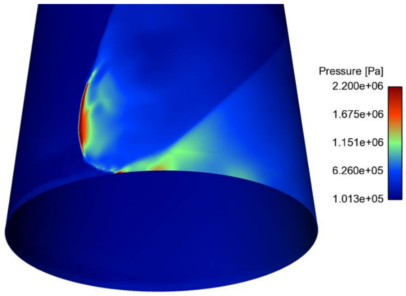

(a) Detonation Structure - Case 1

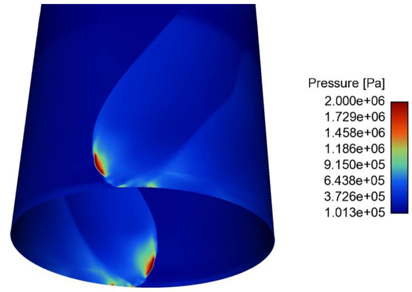

(b) Detonation Structure - Case 2

Figure 2: Instantaneous contours of absolute pressure plotted in Pa on a constant radius (r = 73 [mm]) section of the annulus. The left figure is from Case 1 (Table 1) where one detonation front was observed. The right figure is obtained from Case 2 simulation where two detonation fronts were observed. Detonation wave, oblique shock and the shock wave reflected off the annulus walls, are shown traversing the channel annulus

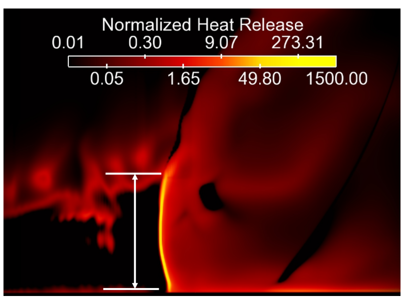

(a) Detonation height - Case 1

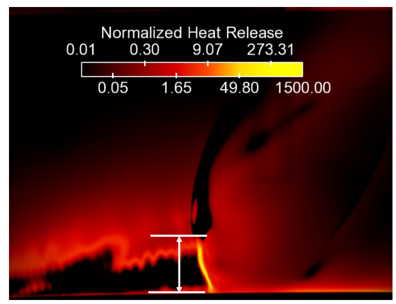

(b) Detonation height - Case 2

Figure 3: Instantaneous contours of normalized reaction heat release plotted in [J m^3/(kg s)] on a log scale. The left figure is from Case 1 (Table 1) where one detonation front was observed. The right figure is obtained from Case 2 simulation where two detonation fronts were observed. Reduced Detonation height a consequence of reduced fill and multiple detonation fronts can be clearly observed. Simulated detonation height, Case 1 ≈ 38 mm & Case 2 ≈ 18 mm

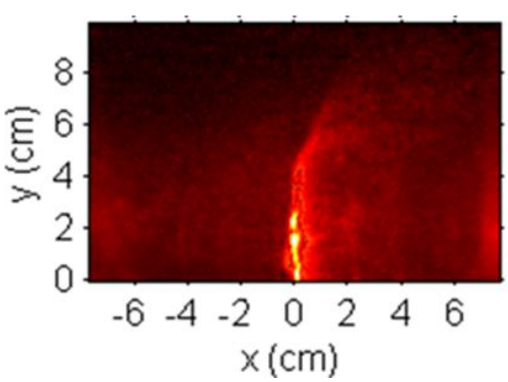

(a) Case 1

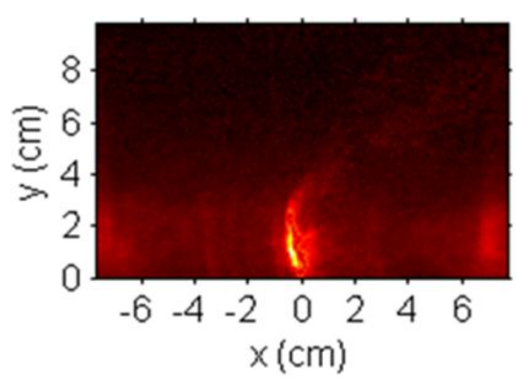

(b) Case 2

Figure 4: Contours of OH^* chemiluminescence obtained from experiments performed at AFRL [5].

the main fuel-air jet. These fuel-rich ligaments preferentially increase the un-mixedness in the downstream regions

of the channel annulus.
In order to look into mixing quality a variable known as unmixedness [13] quantifying the mixing between fuel and air, can be computed using the Bilger mixture fraction. The unmixedness is defined as the following

$$Unmix = \frac{\overline{Z''^2}}{\bar{Z}\left(1-\bar{Z}\right)} \tag{1}$$

where averaging operation, denoted by the bar, is performed in the circumferential direction.

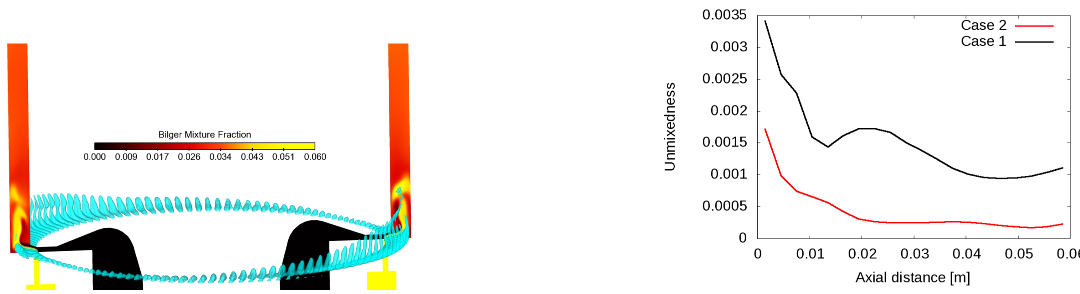

(a) Contours of Bilger mixture fraction

(b) Unmixedness - Case 1 & 2

Figure 5: The left shows the contours and iso-surface (Z = 0.06) of Bilger mixture fraction from Case 2 (Table 1) where two detonation fronts were observed. The right figure compares the unmixedness of fuel-air mixture from simulations of Case 1 and 2.

The pinching of rich fuel-air ligaments can be clearly observed in Fig. 5b, where for the Case 1 the unmixedness of the mixture is increased at an axial location of 0.02[m]. Interestingly, the Case 2 simulations, where two detonations were observed, shows better mixing profile compared to the results from Case 1. This increase in mixing efficiency could be attributed to the increased turbulence generation caused by the increased air & fuel flow rate and also due to the presence of the second detonation front. Similar effect of increased vorticity and velocity fluctuations behind detonation fronts have been observed in other studies [14]. This effect will be investigated in more detail in the future studies.
Due to the preferential concentration of fuel-air mixture towards the outer annulus wall, the detonation fronts in both Case 1 and Case 2 are also observed to stabilize closer to the outer wall. Figure 6 show the instantaneous contours of absolute pressure plotted on an axial cross section of the annulus channel for both Case 1 and Case 2.

5 Summary

Results from three-dimensional simulations of a H2-air atmospheric rotating detonation combustor (RDC) are presented in this study. Starting from an ignition kernel in the initiator tube unsteady simulations are performed in a way to reflect the operation of the RDC in the experimental studies. Focus of this study is devoted towards understanding: a) Detonation diffraction from the initiator tube into the channel annulus, b) Influence of fill height and bifurcation of detonation into multiple fronts, and c) Impact of mixing on detonation stabilization.

6 Acknowledgment

Authors would like to thank Dr. Brent Rankin (AFRL) for sharing the experimental data and the relevant geometric configuration. The authors would also like to thank Dr. A. J. Dean, Dr. N. D. Joshi, Dr. M. Peter, Mr. Owen Rickey for productive discussions and for their help with simulations.

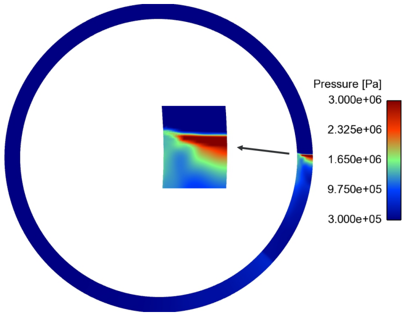

(a) Detonation Structure - Case 1

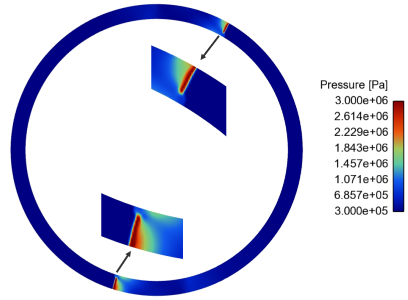

(b) Detonation Structure - Case 2

Figure 6: Instantaneous contours of absolute pressure plotted in [Pa]. The left figure is from Case 1 (Table 1) where one detonation front was observed. The right figure is obtained from Case 2 simulation where two detonation fronts were observed. Detonation stabilization is observed on the outer combustor wall consistent with mixing profile observed in Fig. 5a.

References

[1] Wolański, Piotr, Detonative propulsion, Proceedings of the combustion Institute, 34, 1, 125–158, 2013, Elsevier.

[2] Kailasanath, K, Recent Developments in the Research on Rotating-Detonation-Wave Engines, 55th AIAA Aerospace Sciences Meeting, 0784, 2017.

[3] Rui Zhou and Dan Wu and Jianping Wang, Progress of continuously rotating detonation engines, Chinese Journal of Aeronautics , 29, 1, 15 - 29, 2016.

[4] Rankin, Brent A and Fotia, Matthew L and Paxson, Daniel E and Hoke, John L and Schauer, Frederick R, Experimental and numerical evaluation of pressure gain combustion in a rotating detonation engine, 53rd AIAA Aerospace Sciences Meeting, 2015–0877, 2015.

[5] Rankin, Brent A and Richardson, Daniel R and Caswell, Andrew W and Naples, Andrew G and Hoke, John L and Schauer, Frederick R, Chemiluminescence imaging of an optically accessible non-premixed rotating detonation engine, Combustion and Flame, 176, 12–22, 2017, Elsevier.

[6] Cocks, Peter and Holley, Adam T and Rankin, Brent A, High fidelity simulations of a non-premixed rotating detonation engine, 54th AIAA Aerospace Sciences Meeting, 0125, 2016.

[7] Roy, Arnab and Bedick, Clinton and Strakey, Peter and Sidwell, Todd and Ferguson, Don and Sisler, Andrew and Nix, Andrew, Development of a Three-dimensional Transient Wall Heat Transfer Model of a Rotating Detonation Combustor, 54th AIAA Aerospace Sciences Meeting, 0902, 2016.

[8] ANSYS FLUENT, Theory Guide Documentation, https://support.ansys.com/AnsysCustomerPortal/, ANSYS Inc., ANSYS Fluent, R17, 2015

[9] Ó Conaire, Marcus and Curran, Henry J and Simmie, John M and Pitz, William J and Westbrook, Charles K, A comprehensive modeling study of hydrogen oxidation, International journal of chemical kinetics, 36, 11, 603–622, 2004, Wiley Online Library.

[10] Zhou, R and Wang, J-P, Numerical investigation of shock wave reflections near the head ends of rotating detonation engines, Shock Waves, 23, 5, 461–472, 2013, Springer.

[11] Miller, Stephen J and King, Paul I and Schauer, Frederick R and Hoke, John L, Ignition design for a rotating detonation engine, Proceedings of 51st AIAA aerospace sciences meeting including the new horizons forum and aerospace exposition, 7–10, 2013.

[12] Bilger, RW and Stårner, SH and Kee, RJ, On reduced mechanisms for methane air combustion in nonpremixed flames, Combustion and Flame, 80, 2, 135–149, 1990, Elsevier.

[13] Dimotakis, Paul E and Miller, Paul L, Some consequences of the boundedness of scalar fluctuations, Physics of Fluids A: Fluid Dynamics (1989-1993), 2, 11, 1919–1920, 1990, AIP Publishing.

[14] Jin, Tai and Luo, Kun and Dai, Qi and Fan, Jianren, Simulations of Cellular Detonation Interaction with Turbulent Flows, AIAA Journal, 54, 2, 419–433, 2015, American Institute of Aeronautics and Astronautics.